This article has been accepted for publication in IEEE Transactions on Electron Devices. This is the author's version which has not been fully edited and content may change prior to final publication. Citation information: DOI 10.1109/TED.2024.3409202

Reverse Leakage Current Hysteresis in GaN Schottky Barrier Diodes Interpreted in Terms of a Trap Energy Band

R. A. Peña, B. Orfao, I. Íñiguez-de-la-Torre, G. Paz, M. A. Daher, Y. Roelens, M. Zaknoune, J. Mateos, T. González, B. G. Vasallo, and S. Pérez

Abstract—**The hysteresis cycles observed in the reverse leakage current measured at low temperatures in GaN-on-Sapphire Schottky Barrier Diodes (SBDs) have been deeply studied and interpreted in terms of trap-assisted tunneling compatible with the existence of a trap energy band near the metal-semiconductor interface. The analysis of the energies for which the maximum tunneling current occurs, both direct and through this trap band, allows us to explain the behaviors found at different temperatures. Starting from empty trap states by previous illumination, transient current measurements performed under different preconditioning voltages evidence a progressive partial filling/release of the trap energy levels, confirmed as well by pulsed measurements. Captured/released electrons modify the number of trap states available for tunneling and thus the current level. As a consequence, tunneling processes in the go and return paths take place through levels with different occupation within the trap energy band, originating the hysteresis cycle.**

***Index Terms*—Cryogenic temperatures, GaN technologies, hysteresis cycles, Schottky Barrier Diodes, traps.**

I. Introduction

Wide bandgap semiconductors are increasingly being used in high-power applications to overcome limitations such as the relatively low breakdown voltage and thermal conductivity existing in the dominant current technologies as GaAs [1]. In particular, GaN devices are suitable for the next generation of high-frequency, high-power circuits [2-5], since the use of this wide-bandgap semiconductor may reduce the size and complexity of frequency multipliers and mixers. Specifically, GaN Schottky barrier diodes (SBDs) are excellent candidates for the fabrication of sources and detectors operating in the sub-mm wave range. They could further optimize applications in medical imaging, spaceborne earth observation, planetary science missions, etc., as well as those requiring high-speed communications [6]. Some of these circuits need to operate not only at room temperature or above, but also in cryogenic environments [7]; thus, these technologies must be carefully analyzed at such low temperatures. However, there are drawbacks to be overcome for their practical use, as the high level of leakage current exhibited by GaN SBDs. In particular, the existence of traps at the metal-semiconductor interface involves the appearance of extra conductance components in addition to those of the ideal device [8-11].

In a recent work, we measured DC *I-V* curves of GaN-on-Sapphire SBDs which revealed the presence of hysteresis cycles at low temperatures under reverse bias, which were preliminarily interpreted in terms of the presence of two different trap levels originating trap assisted tunnelling (TAT) [12]. Hysteretic behaviours, as well attributed to trap effects, have also been detected in other devices, like at the gate contact of GaN heterostructure-based p-FETs [13-15]. However, an exhaustive analysis of the low-temperature trap-related mechanisms at the origin of the observed hysteresis in GaN SBDs phenomena is still lacking. In this work, detailed DC and pulsed *I-V* curves, as well current transients, were measured in a wide temperature range (from 33 to 475 K), in the dark and under illumination conditions, on large-size GaN-on-Sapphire SBDs. Hysteresis cycles were observed under operating conditions similar to those in Ref. 12, but exhibiting a smoother transition between TAT regimes dominated by different trap energies. Our comprehensive analysis allows us to interpret the hysteresis as originated by traps spread over an energy band rather than at two single levels. Trap energy bands (TEBs) have also been considered to explain the behavior of the leakage current in other GaN devices [16-18]. In our devices, the progressive occupation of traps at different energies within the TEB explains the evolution of the current level in the "go" and "return" paths of the hysteresis cycles.

In addition, other effects as the lowering of the effective Schottky barrier height for decreasing temperatures, typically attributed to barrier inhomogeneities and/or leakage currents [19],[20], as in the case of GaAs

This work has been partially supported through Grant PID2020-115842RB-I00 funded by MCIN/AEI/10.13039/501100011033, by Grant No. SA136P23 by Junta de Castilla y León and FEDER and by French project ShoGaN (No. ANR-17-CE24-0034). R. A. Peña acknowledges the "Investigo" contract funded by the Junta de Castilla y León and by "European Union NextGenerationEU/PRTR.

R. A. Peña, I. Íñiguez-de-la-Torre, G. Paz, J. Mateos, T. González, B. G. Vasallo, and S. Pérez are with the Applied Physics Department and USAL-NANOLAB, University of Salamanca, E-37008 Salamanca, Spain.

B. Orfao was with the Applied Physics Department and USAL-NANOLAB, University of Salamanca, E-37008 Salamanca, Spain. She is now with Institut d'Électronique, de Microélectronique et de Nanotechnologie (IEMN), France.

M. A. Daher, Y. Roelens, and M. Zaknoune are with Institut d'Électronique, de Microélectronique et de Nanotechnologie (IEMN), France.

This article has been accepted for publication in IEEE Transactions on Electron Devices. This is the author's version which has not been fully edited and content may change prior to final publication. Citation information: DOI 10.1109/TED.2024.3409202

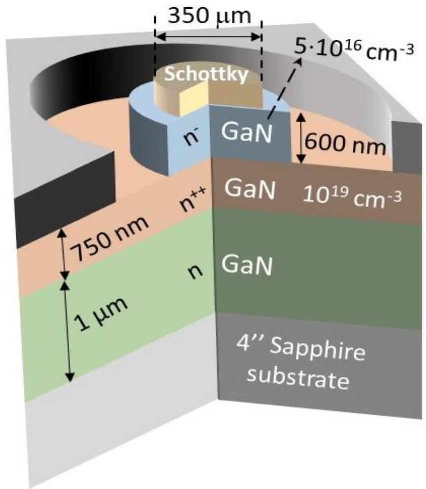

Fig. 1. Sketch of the GaN Schottky barrier diode geometry.

technologies [21],[22], could also be explained in terms of the trapping mechanisms.

This paper is organized as follows. In Section II, we describe the devices and the set-up used to carry out the measurements. We also include an overview of a physical model that allows us to calculate ideal SBD currents. In Section III, the measurements and results of simulations are discussed to explain the temperature and voltage dependence of the hysteresis effect in terms of the mentioned TEB. Finally, the main conclusions of our work are presented in Section IV.

II. DEVICES, EXPERIMENTAL SETUP AND PHYSICAL MODEL

The GaN SBDs under study have been fabricated at IEMN with the epitaxial layer sketched in Fig. 1. They were grown by metal organic chemical vapor deposition (MOCVD) on Sapphire substrate. The epilayer included a 750 nm thick n^{++} (10^{19} cm^{-3}) GaN layer to achieve low series resistance and a 600 nm n^{-} (nominally 5×10^{16} cm^{-3}) GaN as active layer. Ti/Al/Ni/Au ohmic contacts were fabricated with a typical lift-off technique and annealed at 850°C for 30". A SiO_2 hard mask was used to define the Schottky mesa. Then, a bi-layer e-beam lithography process was used, and the Pt/Au Schottky electrode was deposited by e-beam evaporation. This study focuses on a 350 μm-diameter diode, where edge effects can be considered as negligible thanks to its large size [23]. Other diodes of different (large) sizes exhibit similar behavior and the conclusions of this work can be extended to them.

Temperature measurements in a range from 33 to 475 K were carried out by means of a LakeShore CRX-VF cryogenic probe station. The DC pulsed and transient *I-V* measurements were done by means of a Keithley 4200-SCS semiconductor analyser connected to the device through variable temperature probes. Additional room temperature *C-V* measurements were performed to determine the effective doping concentration N_D of the epilayer by means of an Agilent E4980A precision LCR meter. A doping level N_D=3.8×10^{16} cm^{-3} was extracted from these measurements.

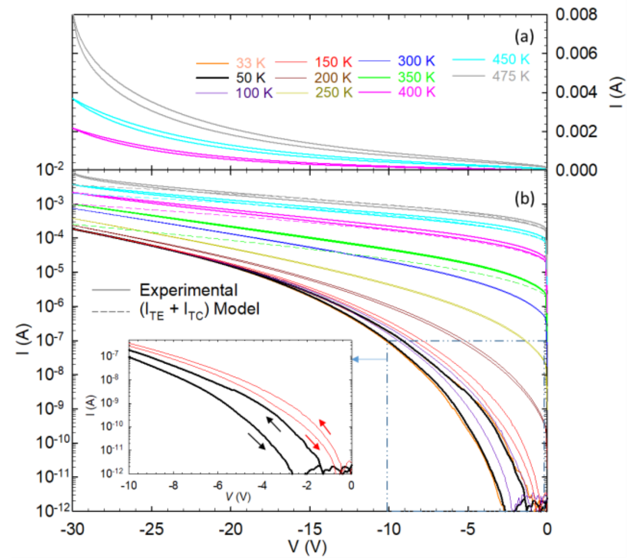

Fig. 2. *I-V* reverse-bias curves measured in dual sweep mode (solid lines), represented: (a) in linear scale for the highest temperatures (400 K to 475 K) and (b) in logarithmic scale from 33 K to 475 K, compared with the theoretical model (dashed lines, including $I_{TE}+I_{TC}$). Inset: hysteresis loops in the *I-V* curves for 50 and 150 K.

From the forward *I-V* curves, a Schottky barrier height ϕ_B of around 0.68 eV and a series resistance R_s of around 0.49 Ω were obtained for the highest temperatures.

To analyse the results of the measurements, we make use of a physical model which allows us to calculate the ideal reverse leakage current components in the SBD and identify the energy levels at which the maximum tunnel injection occurs [24]. In reverse bias, we consider the thermionic emission J_{TE} and the direct tunnelling currents J_{TC} due to electrons traveling from the metal to the semiconductor, being the ideal reverse current density J_{rev}=J_{TE}+J_{TC}.

The model addresses both thermionic and tunneling current components, and both forward and reverse polarities, in a unified way and with the same set of parameters. As detailed in [24], the general expression of the current density in a $d\varepsilon$ energy interval around a given energy ε is given by $J(\varepsilon)d\varepsilon = -e\cdot N_{m,s}(\varepsilon)\cdot T_C(\varepsilon)d\varepsilon$, where $N_{m,s}(\varepsilon)$ is the rate of incident electrons from the metal to the semiconductor and $T_C(\varepsilon)$ is the transmission coefficient, both at energy ε. J_{TC} and J_{TE} are calculated by integrating $J(\varepsilon)$ over the appropriate electron energy interval susceptible to contribute to the respective current. The transmission coefficient involved in J_{TC} is estimated by means of the Wentzel–Kramers–Brillouin approximation as $T_c(\varepsilon) = \exp\left[-\frac{2}{\hbar}\int_{x_1}^{x_2}\sqrt{2m^*(\varepsilon_c(x)-\varepsilon)}dx\right]$, where x_1 and x_2 are the classical turning points, $\hbar$ is the reduced Planck's constant and $\varepsilon_c(x)$ the barrier energy profile, which includes the effect of image force lowering. In the case of J_{TE} the transmission coefficient is exactly 1. Real effects, like the influence of the series resistance R_s and the ideality factor η, are incorporated to the resulting expression in forward bias. The model is based on six parameters: N_D, obtained from the *C-V* measurements; the effective mass of

This article has been accepted for publication in IEEE Transactions on Electron Devices. This is the author's version which has not been fully edited and content may change prior to final publication. Citation information: DOI 10.1109/TED.2024.3409202

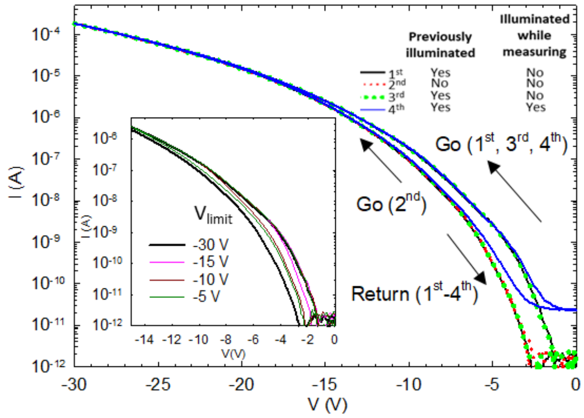

Fig. 3. DC dual sweep reverse bias measurements at 50 K in dark conditions (1st, 2nd, and 3rd measurements) and under illumination (4th). It has to be noted that 1st and 3rd measurements are done after the device has been illuminated. Inset: hysteresis cycles for different maximum values of the reverse bias cycle (V_{limit}) of -30, -15, -10 and -5 V.

electrons m^*=0.22m_0 and the permittivity ε_s=8.9ε_0, both taken from the literature for the case of GaN; and ϕ_B, R_s and η, extracted from the fitting of the forward-bias *I-V* curves and then used to predict the reverse-bias behavior ($J_{rev}=J_{TE}+J_{TC}$) without any further adjustment. A thorough description of the model can be found in [24].

III. Results and Discussion

a. DC characterization

The reverse-bias *I-V* characteristics of the 350 µm-diameter SBD under analysis measured from 33 to 475 K are plotted in Fig. 2. At the lower temperatures, significant hysteresis cycles are revealed by the DC dual voltage sweep when plotted in logarithmic scale in Fig. 2(b), which tend to disappear or are quite reduced above 200 K, as observed for the highest temperatures in the linear-scale plot of Fig. 2(a). We note that *C-V* measurements were also made in this technology at different temperatures and no hysteretic behaviour was observed.

To illustrate the observed *I-V* hysteretic phenomenon, Fig. 3 presents dual sweep *I-V* curves, measured at 50 K from V= 0 V to V_{limit}=-30 V ("go") and return from V_{limit} =-30 V to V=0 V ("return") with the device under different illumination conditions. Under these low temperature conditions, a well-defined hysteresis cycle is observed. The first measurement (black line) was done while keeping the device in dark conditions, but after previous illumination. In this first case, a hysteresis cycle is evidenced by a decrease of the leakage current during the "return" sweep. After this first cycle, the hysteresis phenomenon vanishes when the measurements are repeated in dark conditions: all the resulting *I-V* curves follow the lower return branch of the initial sweep (red dots). However, the initial response can be recovered after a new illumination of the device (green dots), leading an analogous *I-V* behaviour as in the first case described before. Thus, the whole process can be experimentally repeated. Finally, the dual sweep *I-V* has been measured under illumination (blue line). In this case, the current level is higher for the lower voltages, but, essentially, the hysteresis cycle follows the first case (dark conditions but after illuminating the device).

The inset of Fig. 3 shows the different hysteresis cycles for four different maximum values of the reverse bias at 50 K: V_{limit}=-5 V, -10 V, -15 V and -30 V. The width of the hysteresis cycle becomes wider when the absolute value of V_{limit} is increased.

In Fig. 2, we have also compared the experimental data with the *I-V* values obtained with the ideal model referenced before. The modelled values (dashed lines) correctly fit measurements for T > 350 K. However, for lower temperatures, an excess current appears in the experimental curves with respect to the ideal levels, and thus the model is no longer valid. To explain the difference between the measurements and the modelled *I-V* characteristics, the excess leakage-current density, calculated as $J_{\text{excess}}=J_{\text{exp}}-(J_{\text{TE}}+J_{\text{TC}})$, being J_{exp} the experimental current density, has been evaluated. Usually, this excess current is attributed to traps or inhomogeneities in the epilayer or at the interface [11,12]. In our case, and particularly for T<150 K, J_{excess} very weakly depends on temperature, indicating that the dominant mechanism at the origin of this behaviour is trap-assisted tunnelling (TAT), rather than other mechanisms exhibiting a strong temperature dependence like Poole-Frenkel emission or variable range hopping [8].

To identify the TAT processes present in the SBD, Fig. 4 shows the values of ln (J_{excess}) as a function of the inverse of the surface electric field E for the "go" branch of the 1st measurement for T=33 K and 50 K, as well as for the "return" path common to both cycles and all the others plotted in Fig. 3. The linear behavior of such plots confirms the presence of TAT processes, whose associate leakage current depends on the electric field as [8]:

$$J_{TAT} \propto \exp\left(-\frac{4\sqrt{2qm^*\phi_t^3}}{3\hbar E}\right), \qquad (1)$$

where $\hbar$ is the Planck constant and ϕ_t is the trap energy level.

There are at least two identifiable trap energy levels in the plot of Fig. 4: ϕ_{t1}=0.23 eV (TAT_1) and ϕ_{t2}=0.38 eV (TAT_2). Interestingly, while for the "return" path the experimental data agree reasonably well with the presence of just one trap with an energy level of ϕ_{t2}=0.38 eV, the "go" branch reflects the presence of different traps' energies. Indeed, from about -6 V, the slope of the "go" path progressively changes from an energy around ϕ_{t1}=0.23 eV to a final value about ϕ_{t2}=0.38 eV, which then dominates in the "return" path.

This article has been accepted for publication in IEEE Transactions on Electron Devices. This is the author's version which has not been fully edited and content may change prior to final publication. Citation information: DOI 10.1109/TED.2024.3409202

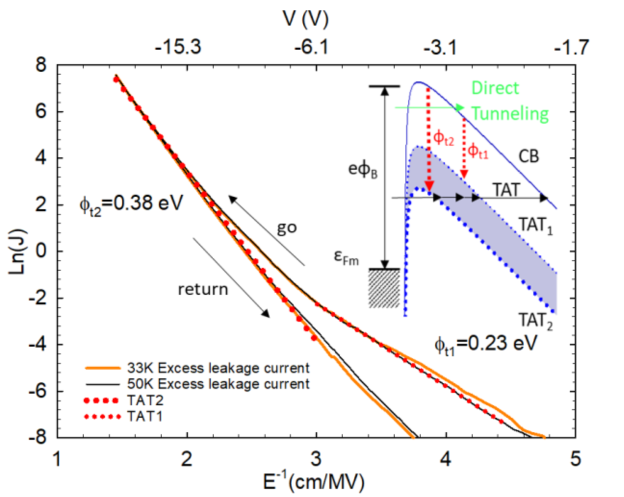

Fig. 4. Excess leakage current density of the 1st measurement as a function of the inverse of the surface electric field for T= 30 K and 50 K. Linear fitting dots for both the initial "go" (red thin dots) and "return" (red thick dots) paths are also plotted, providing values of trap energies of TAT processes of ϕ_{t1}=0.23 eV and ϕ_{t2}=0.38 eV, respectively. Inset: schematic diagram illustrating the energy bands at the Schottky metal/semiconductor interface.

b. Pulsed and Transient Measurements

To better understand the influence of the trap levels identified in Fig. 4 and to link it with that shown in Fig. 3, pulsed *I-V* curves were obtained. Once the device was illuminated, the current was measured with base voltages of V_{base}=0 V and -15 V, being the pulse width and period of 10 ms and 1 s, respectively. Fig. 5(a) presents the dark pulsed *I-V* curves measured at 50 K after illuminating the device (as in the first case in Fig. 3). When V_{base}=0 V, the current response is the same as in the DC hysteresis cycle both in the "go" and "return" pulsed sweeps, whereas if just after illuminating V_{base}=-15 V is applied, the measured current level in both pulsed sweeps corresponds to the low branch of the DC cycle (DC "return" path). These results indicate that, irrespectively of the fact that the *I-V* curve is measured in a pulsed way or not, the application of high reverse voltages (either as V_{base} or bias amplitude) induce a long-lasting occupation of the traps (mainly ϕ_{t1}, as observed in Fig. 4) which reduces the current level and makes the current follow the behavior dominated by the ϕ_{t2} level, as identified in Fig. 4.

To confirm this observation and better recognize the different current mechanisms in the "go" and the "return" paths and thus gain more insight into the physical origin of hysteresis, Fig. 5(b) presents the current transient measured at 50 K when applying a bias of V=-7.5 V subsequently to, first, the illumination of the device and, second, the application (in dark) of a preconditioning voltage V_{pre} for a long enough time. Again, two different values of V_{pre} are considered (high and low, the same as those of V_{base} in the pulsed measurements). In the case of V_{pre}=0 V, a capture transient involving a decreasing value of current is identified (red curve in Fig. 5(b)). This can be interpreted as

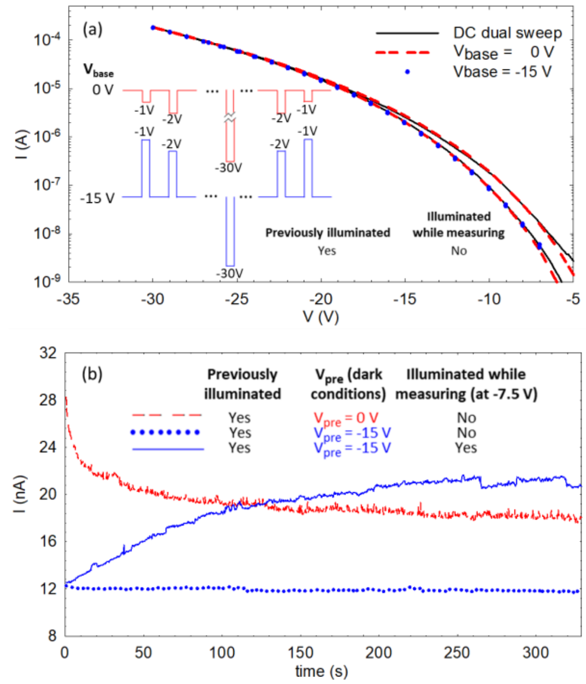

Fig. 5 (a) Dark pulsed *I-V* measurements at 50 K performed after the device has been illuminated with base voltages V_{base} of 0 V and -15 V. Pulse width and period are 10 ms and 1 s, respectively. The DC dual sweep (black line) is plotted for comparison. Inset: scheme of the time-dependent applied voltage. (b) Current transient measurements at 50 K made with V=-7.5 V. A preconditioning voltage V_{pre} was also applied before the measurements (after illumination of the device). The solid-blue curve was obtained under illumination, while the other two curves were obtained in dark conditions.

following: when illuminating the device, trapped electrons are released and traps remain mostly empty while V_{pre}=0 V is applied. Afterwards, when biasing the SBD with a reverse voltage of V=-7.5 V in dark conditions, as electrons tunnel through the traps, a progressive filling of the corresponding energy levels present in Fig. 4 (mainly ϕ_{t1}) takes place, making less probable the tunnelling of subsequent electrons. Thus, the current level decreases with time due to the lower number of available trap states to tunnel through them.

On the other hand, when the preconditioning voltage is V_{pre}=-15 V, most of the states are filled before the measurement at V=-7.5 V is carried out. As a result, a low-level current practically constant in time is obtained (Fig. 5(b), blue dots), indicating that the release of electrons from the traps takes times longer than 320 s. However, the current level continues to be higher than the ideal one associated to direct tunneling, indicating that not all the trap energy states are filled, those at ϕ_{t2} remaining partially empty as revealed by Fig. 4. This is in good agreement with the fact that the hysteresis cycle broadens when the maximum value of the reverse bias cycle V_{limit} is increased, since the occupation of the trap levels is also increased (inset of Fig. 3). In addition, if after applying V_{pre}=-15 V in dark conditions, the device is kept under illumination, when measuring at V=-7.5 V, the current level increases because the illumination contributes to release the traps in shorter

This article has been accepted for publication in IEEE Transactions on Electron Devices. This is the author's version which has not been fully edited and content may change prior to final publication. Citation information: DOI 10.1109/TED.2024.3409202

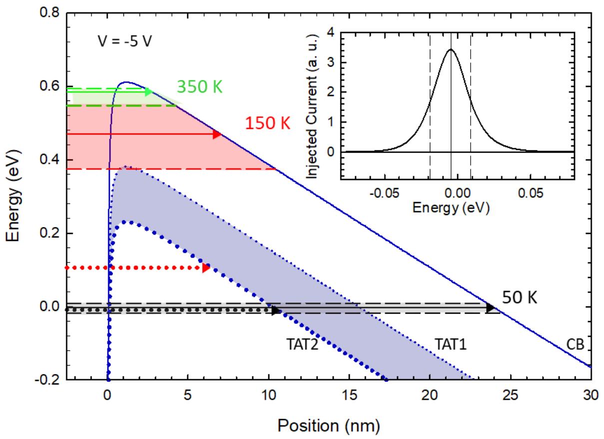

Fig.6. Semiconductor conduction band and TEB near the Schottky contact for V=-5 V. The energies at which the maximum tunnel injection from metal to TEB occurs are indicated by dotted arrows, in grey for 50 K and red for 150 K. The energy ranges at which the maximum direct tunnel injection from metal to semiconductor occurs are shaded in grey for 50 K, red for 150 K and green for 350 K. The energy at with the maximum direct injection takes place is indicated by a solid arrow and those corresponding to half the maximum value by dashed lines. The origin of energies is the Fermi level in the metal. Inset: direct tunnelling current injection as function of energy at 50 K, with the previously mentioned energies marked by vertical lines.

times, which enhances the TAT processes (solid-blue curve in Fig. 5(b)).

The previous results indicate that the *I-V* hysteresis should be caused by the bias-induced occupation of the trap states near the metal-semiconductor interface, which hinders the injection of electrons into the semiconductor by TAT. The behaviour of the slope observed for the excess leakage current density in Fig. 4 suggests that these devices, rather than two types of traps located at a different energy level, have a band of trap energies located between ϕ_{t1}=0.23 eV and ϕ_{t2}=0.38 eV, similar to the band found in [16-18]. Trap states are numerous enough and present so close energies that form an energy band. This band of traps has been depicted in the inset of Fig. 4 together with the conduction band in the Schottky contact; the black arrows indicate the electrons going from the metal to the semiconductor conduction band assisted by TAT mechanisms.

C. Physical Interpretation in Terms of a Trap Energy Band (TEB)

To study in detail the role played by this TEB, we have calculated with the ideal model the energies for which the maximum direct tunnelling current injection occurs. Fig. 6 shows the conduction band of the semiconductor and the TEB near the Schottky contact at *V*=-5 V. In the inset, the injected direct tunnelling current density as function of energy at 50 K obtained with the ideal model is represented, where the energy for the maximum injection is marked by a vertical solid line and the energies where the injection is half the value of the maximum injected current by dashed lines. As these values delimit the principal contribution of direct injected carriers, this range is also signalled in the main figure (black lines) to compare the energy values for injection and the position of the TEB, since if the direct current has a preferred path which overlaps with trap levels, the probability of filling these traps is higher than otherwise.

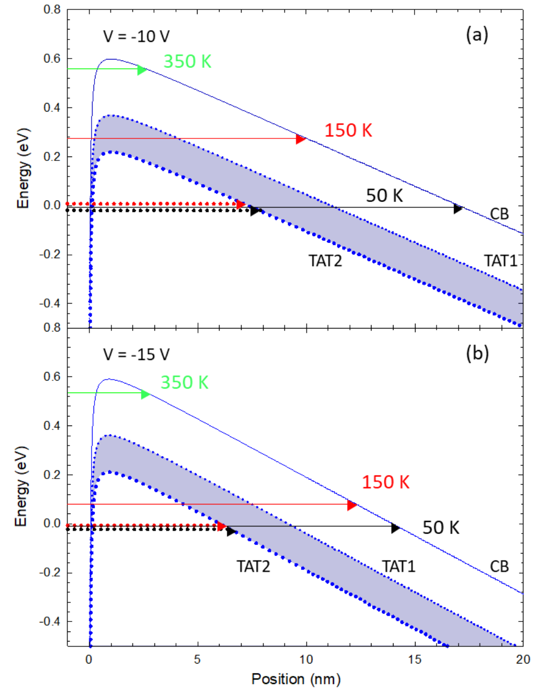

Fig. 7. Semiconductor conduction band and TEB near the Schottky contact, and energies at which the maximum direct tunnel injection occurs at 50 K, 150 K, and 350 K for applied voltages *V* (a) -10 V and (b) -15 V. The energies at which the maximum tunnel injection from the metal to the TEB occurs are also indicated by dotted arrows.

At 50 K, according to Fig. 6, direct tunnelling injection occurs at energies around 0 eV, corresponding to the Fermi level of the metal. At this point, it is easier for electrons to reach the semiconductor conduction band by TAT mechanisms through the band of traps. The capture of electrons by the traps may explain both the transient measurements of Fig. 5(b) and the hysteresis in the *I-V* curve observed in Figs. 3 and 4. Trap states, if initially empty by illumination, may capture passing electrons while tunnelling, which would cause a reduction with time in the current level as that observed in the capture transient (with V_{pre}=0 V) shown in Fig. 5(b), since the empty trap states available for tunnelling decrease.

As concerns the hysteresis cycle, at low reverse bias, with trap states empty by the previous illumination, electrons tunnelling to the physically closer trap state at ϕ_{t2}=0.38 eV (TAT_2) can easily reach the energy level ϕ_{t1}=0.23 eV of TAT_1, since there is a continuity of states between them in the TEB. As a consequence, the trap effective energy revealed by the device is 0.23 eV (TAT_1 level), as observed in the “go curve” of Fig. 4 for low electric fields (TAT path depicted in the inset).

Since electrons reach the TEB through the lower TAT_2 level, to assist the interpretation we have also identified with the ideal model the energy at which maximum tunnel

This article has been accepted for publication in IEEE Transactions on Electron Devices. This is the author's version which has not been fully edited and content may change prior to final publication. Citation information: DOI 10.1109/TED.2024.3409202

injection occurs from the metal to the TEB (assumed to be empty). To this end, we consider as profile of the energy barrier that corresponding to the TAT_2 level (thick dotted line in Fig. 6), calculated subtracting ϕ_{t2} to the energy of the semiconductor conduction band. As observed, at 50 K the maximum injection to the TEB takes place also at energies around the Fermi level.

When increasing the reverse bias, direct tunnel injection still occurs at energies around 0 eV but with higher intensity (black arrows in Fig. 7), so that the probability of filling the traps is enhanced. In particular, trap states close to ϕ_{t1} will be filled earlier and this would explain the progressive change in the slope of the "go path" in Fig. 4 for intermediate fields, with the associated trap energies changing from ϕ_{t1}=0.23 eV to ϕ_{t2}=0.38 eV.

Finally, for higher fields, the maximum probability for the electrons to find unoccupied traps takes place at the level of TAT_2 (ϕ_{t2}=0.38 eV), which determines the slope. In the "return path" of the dual sweep cycle in Fig. 4, since the release time of the traps is quite long (see transient in Fig. 5(b) for V_{pre}=-15 V), a large number of trap states remain occupied, mainly around TAT_1, so that the current level is lower, and the slope is dominated by traps close to TAT_2. The longer distance between the free trap states (TAT_2) and the conduction band of the semiconductor also contributes to reduce the current level.

The energy values for the principal injection contribution at 150 K (red solid arrow) and 350 K (green solid arrow) are also plotted in Fig. 6. At these higher temperatures, the injection occurs near the top or above the trap energy band, which implies less influence of the traps and then a reduced (or nearly missing) hysteresis cycle, in accordance with the experimental measurements, especially at 350 K, temperature at which the leakage current is close to the ideal values. In the case of 150 K, the situation is intermediate, since, despite direct tunnelling through the conduction band hardly overlaps with the trap states (red shaded path in Fig. 6), tunnelling to the TEB (red dotted arrow) is significant and leads to the observed hysteresis in the inset of Fig. 2, less pronounced than at 50 K due to the larger contribution of direct tunnelling.

To confirm the previous interpretation, Fig. 7 represents the energies where the maximum injection (both direct and through the TEB) occurs for other two voltages, *V*=-10 V and -15 V, at the same temperatures considered before (50 K, 150 K and 350 K). At 50 K, for the three voltages the maximum direct current injection occurs at energies where there are accessible traps states to assist tunnelling, whereas for the highest temperature, 350 K, it happens the opposite, the maximum direct injection takes place mainly above the TEB. At 150 K, to have a significant overlap of the maximum direct injection region with the TEB, negative voltages higher than -10 V must be applied, which justifies that the influence of the traps is less than for 50 K but higher than for 350 K. In addition, it should be noted that at this temperature some electrons can be released from the traps by thermal emission phenomena (like Poole-Frenkel mechanisms) and which can lead to an enhancement of TAT due to an increase in the density of unoccupied traps. This would agree with the fact that the width of the hysteresis cycle at 150 K is narrower than that obtained at 50 K, see inset of Fig. 2. Focusing on the tunnelling from the metal to the TEB, it is remarkable that the energies of the maximum injection for 50 K and 150 K are both close to the Fermi level, thus leading to more similar current levels as the bias increases, as observed in measurements.

The different influence of the trapping band on the electron dynamics as a function of temperature discussed above may also be at the origin of the reduction in Schottky barrier height estimated from the forward bias *I-V* measurements typically found at low temperatures [19]. This is due to the fact that, even in forward bias, tunnelling processes may be significant, since when the importance of the TEB increases, the effective Schottky barrier height is lower.

IV. Conclusions

The reverse leakage current behavior has been analysed in depth for very low temperatures in edge-effect-free GaN-on-Sapphire SBDs. *I-V-T* measurements show the presence of hysteresis effects. The comparison between the measurements and an ideal physical model accounting for thermionic emission and direct tunnelling current suggests that TAT dominates the leakage current at low temperature, since the excess leakage current shows a very weak dependence on temperature. We ascribe the origin of the hysteresis to the bias-induced filling of traps spread over an energy band near the metal-semiconductor interface between values of around 0.23 eV and 0.38 eV. The analysis of the energies for which the maximum direct and through-TEB tunnelling current occurs justifies the higher influence of the traps at the lowest temperatures, with the correspondent hysteretic behavior. This theory is reinforced by transient/pulsed-DC measurements carried out with different preconditioning/base voltages.

References

[1] I. Mehdi, J. V. Siles, C. Lee, and E. Schlecht, "THz diode technology: Status, prospects, and applications," in Proceedings of the IEEE, vol. 105, p. 6, 2017.
[2] K. Dang et al., "A 5.8-GHz high-power and high-efficiency rectifier circuit with lateral GaN Schottky diode for wireless power transfer," *IEEE Trans. Power Electron.*, vol. 35, nº 3, pp. 2247--2252, 2019.
[3] H. Amano et al., "The 2018 GaN power electronics roadmap," *J. Phys. D: Appl. Phys.* , vol. 51, nº16, p.163001, 2018.
[4] T. J. Flack, B. N. Pushpakaran and S. B. Bayne, "GaN Technology for Power Electronic Applications: A Review," *J. Electron. Mater.*, vol. 45, pp. 2673-2682, 2016.
[5] F. Roccaforte, P. Fiorenza, G. Greco, R. Lo Nigro, F. Giannazzo, F. Iucolano and M. Saggio, "Emerging trends in wide band gap semiconductors (SiC and GaN) technology for power devices," *Microelectron. Eng.*, vol. 187, pp. 66-77, 2018.
[6] K. Hoo Teo et al., "Emerging GaN technologies for power, RF, digital, and quantum computing applications: Recent advances and prospects," *J. Appl. Phys.*, vol. 130, no 16, 2021.
[7] K. Jacob et al., "Characterization of the 530-625 GHz receiver unit for the Jupiter mission JUICE/SWI," in Proceedings of the

36th ESA Antenna Workshop on Antennas and RF Systems for Space Science, 6 pp., 2015.

[8] K. Fu, H. Fu, X. Huang, T. Yang, C. Cheng, P. R. Peri, H. Chen, J. Montes, C. Yang, J. Zhou, X. Deng, X. Qi, D. J. Smith, S. M. Goodnick, and Y. Zhao, “Reverse leakage analysis for As-grown and regrown vertical GaN-on-GaN Schottky barrier diodes,” *IEEE J. Electron Devices Soc.*, vol. 8, pp. 74-83, 2020.

[9] P. Pipinys and V. Lapeika, “Temperature dependence of reverse-bias leakage current in GaN Schottky diodes as a consequence of phonon-assisted tunneling,” *J. Appl. Phys.*, vol. 99, nº 9, p. 093709, 2006.

[10] E. J. Miller, E. T. Yu, P. Waltereit, and J. S. Speck, “Analysis of reverse-bias leakage current mechanisms in GaN grown by molecular-beam epitaxy,” *Appl. Phys. Lett.*, vol. 84, nº 4, pp. 535-537, 2004.

[11] T. Hashizume, J. Kotani, and H. Hasegawa, “Leakage mechanism in GaN and AlGaN Schottky interfaces,” *Appl. Phys. Lett.*, vol. 84, nº 24, pp. 4884-4886, 2004.

[12] B. Orfao, M. A. Daher, R. A. Peña, B. G. Vasallo, S. Pérez, I. Iñiguez-de-la-Torre, G. Paz-Martínez, J. Mateos, Y. Roelens, M. Zaknoune, and T. González, “Reverse-bias current hysteresis at low temperature in GaN Schottky barrier diodes,” *J. Appl. Phys.*, 135, no. 1, 014501, 2024.

[13] H. Jin et al., “An enhancement-mode GaN p-FET with improved breakdown voltage,” *IEEE Electron Device Lett.*, vol. 43, nº 8, pp. 1191-1194, 2022.

[14] Z. Zheng et al., “Threshold voltage instability of enhancement-mode GaN buried p-channel MOSFETs,” *IEEE Electron Device Lett.*, vol. 42, nº 11, pp. 1584-1587, 2021.

[15] H. Su et al., “Interface state analysis of Schottky-gated p-AlGaN/u-GaN/AlGaN p-FET with negligible hysteresis at high temperatures,” *Appl. Phys. Lett.*, vol. 123, nº 13, 132104(1-6), 2023.

[16] S. Karmalkar, D. M. Sathaiya, and M. S. Shur, “Mechanism of the reverse gate leakage in AlGaN/GaN high electron mobility transistors,” *Appl. Phys. Lett.*, vol. 82, nº 22, pp. 3976-3978, 2003.

[17] J. Racko et al., “A model of trap-assisted tunneling in GaN/AlGaN/GaN heterostructure based on exchange times,” *Appl. Surf. Sci.*, vol. 312, pp. 68-73, 2014.

[18] J. Racko et al., “Simulation of real IV characteristics of metal/GaN/AlGaN heterostructure based on the 12-EXT model of trap-assisted tunnelling,” *Appl. Surf. Sci.*, vol. 395, pp. 122-130, 2017.

[19] T. Maeda, M. Okada, M. Ueno, Y. Yamamoto, T. Kimoto, M. Horita, and J. Suda, “Temperature dependence of barrier height in Ni/n-GaN Schottky barrier diode,” *Appl. Phys. Express*, vol. 10, nº 5, 051002(1-4), 2017.

[20] F. Roccaforte, F. Giannazzo, A. Alberti, M. Spera, M. Cannas, I. Cora, B. Pécz, F. Iucolano and G. Greco, “Barrier inhomogeneity in vertical Schottky diodes on free standing gallium nitride,” *Mater. Sci. Semicond. Process.*, vol. 94, pp. 164-170, 2019.

[21] H. Tecimer, A. Türüt, H. Uslu, Ş. Altındal, and İ. Uslu, “Temperature dependent current-transport mechanism in Au/(Zn-doped) PVA/n-GaAs Schottky barrier diodes (SBDs),” *Sens. Actuator A Phys.*, vol. 199, pp. 194-201, 2013.

[22] M. K. Hudait and S. B. Krupanidhi, “Doping dependence of the barrier height and ideality factor of Au/n-GaAs Schottky diodes at low temperatures,” *Physica B Condens. Matter*, vol. 307, nº 1-4, pp. 125-137, 2001.

[23] B. Orfao, B. G. Vasallo, D. Moro-Melgar, S. Pérez, J. Mateos and T. González, “Analysis of surface charge effects and edge fringing capacitance in planar GaAs and GaN Schottky barrier diodes,” *IEEE Trans. Electron Devices*, vol. 67, nº 9, pp. 3530-3535, 2020.

[24] B. Orfao, G. Di Gioia, B. G. Vasallo, S. Pérez, J. Mateos, Y. Roelens, E. Frayssinet, Y. Cordier, M. Zaknoune, and T. González, “Comprehensive model for ideal reverse leakage current components in Schottky barrier diodes tested in GaN-on-SiC samples,” *J. Appl. Phys.*, vol. 132, no. 4, 044502(1-10), 2022.
.